RESEARCH ARTICLE

Editorial Process: Submission:09/26/2022 Acceptance:07/02/2023

Health and Carcinogenic Risk Assessment of Exposure to by-Products of Photocatalytic Degradation of Toluene in a Spouted Bed Reactor with Porous and Non-Porous Draft Tube

Ghasem Hesam[1], Rezvan Zendehdel[2], Somayeh Farhang Dehghan[1], Hamed Moqtaderi[3], Mohammad Javad Jafari[1]*

Abstract

Objective: This study was performed to assessment the health and carcinogenic risk of exposure to by-products of photocatalytic degradation of toluene in a spouted bed reactor Equipped with porous and non-porous draft tube. **Methods:** For this purpose, titanium dioxide nanoparticles were used as photocatalysts and UV lamps as radiation sources. Degradation efficiency and CO_2 selectivity were compared. By-products were also detected in three spouted bed reactors with and without a porous and non-porous draft tube. **Result:** The results revealed that the degradation efficiency of toluene in the spouted bed reactor without a draft tube was 30.75%. The insertion of porous and non-porous draft tubes in the spouted bed reactor increased the degradation efficiency up to 54.88% and 47.63%, respectively. Meantime, CO2 selectivity decreased from 100% to 50.8% within 180 min irradiation time in the spouted bed reactor without draft tube, while in the spouted bed reactors with porous and non-porous draft tube maintained at 89.85% and 84.35%, respectively. Toluene and four by-products with carcinogenic and non-carcinogenic risk of 0.002176 and 182.2, respectively, were detected in the spouted bed reactors without draft tube. However, no by-products with carcinogenic risk were found in the spouted bed reactor with porous and non-porous draft tube. **Conclusion:** photocatalytic degradation of toluene in a spouted bed reactor without a draft tube produces by-products with health and carcinogenic risks. The insertion of a porous and non-porous draft tube in spouted bed reactors provided mineralization more complete than spouted bed reactor without a draft tube by reducing the dead zone and providing appropriate contact between the toluene, photocatalyst, and UV. Therefore, prevent the formation of dangerous and carcinogenic by-products.

Keywords: Photocatalytic degradation- carcinogenic and non-carcinogenic risk- spouted bed reactor

Asian Pac J Cancer Prev, **24 (7)**, 2245-2252

Introduction

Volatile organic compounds (VOCs) are air pollutants usually found in urban and industrial areas. There is a growing concern about the adverse effects of airborne VOCs on human health (Moradpour et al., 2017). Studies have shown that exposure to VOCs increases the risk of respiratory and cardiovascular disease and even cancers. Thus, it is necessary to control VOCs emission and remove the VOCs from the air (Marchiori et al., 2019; Mohammadi et al., 2020).

Many technologies have been under investigation to removal VOCs from the air such as adsorption (Kumar et al., 2020), filtration (Marycz et al., 2022), catalytic reactions (Chung et al., 2019), negative air ions (Kim et al., 2017), non-thermal plasma (Li et al., 2020), and photocatalytic oxidation (Hesam et al., 2022b). Among these treatments, photocatalytic oxidation (PCO) has attracted ever-increasing attention mainly because of its' great potential in decomposing a broad range of VOCs into CO_2 and H2O under visible and ultraviolet (UV) light in the ambient atmosphere (Yao et al., 2018).

Its capability in removing a wide variety of organic contaminants at room temperature, low-pressure drop, and low energy consumption as well as the stability and safety of the process are among the acknowledged features of the PCO technology (Mamaghani et al., 2018; Mohamed and Awad, 2020). Despite these advantages, still, the generation of unwanted by-products is the main limitation of this advanced technology (Mamaghani et al., 2018).

For a complete PCO reaction, the final products of reactions are CO_2 and H2O. Such a reaction seems perfect for removing VOCs from the air since both CO_2 and H2O are non-dangerous. However, recent studies have found

*[1]Department of Occupational Health and Safety Engineering, School of Public Health and Safety, Shahid Beheshti University of Medical Sciences, Tehran, Iran. [2]Environmental and Occupational Hazard Control Research Center, School of Public Health and Safety, Shahid Beheshti University of Medical Sciences, Tehran, Iran. [3]Department of Mechanical Engineering, Faculty of Engineering, Alzahra University, Tehran, Iran. *For Correspondence: mj.jafari1952@gmail.com*

that the photocatalytic reactions are not as complete as they are assumed to be (Malayeri et al., 2022; Mamaghani et al., 2018; Mo et al., 2013). The photocatalytic oxidation process sometimes stops and produces aldehydes, ketones or organic acids. Some of these unwanted by-products are relatively more harmful to human health than the original contaminants (Mo et al., 2013).

Due to the presence of the aromatic ring in the molecule structure of toluene, PCO degradation of toluene results in a complicated process with the formation of various by-products. It was reported by some authors that benzaldehyde, benzoic acid, benzyl alcohol, and benzene were the first reaction intermediates/by-products of toluene degradation in PCO that some of them can be more toxic and harmful to human health than toluene (Bianchi et al., 2014; Malayeri et al., 2022). These preliminary intermediates can break down through further oxidation and generate various chemical groups of VOCs, namely, aldehydes, alkanes, acids, and alcohols (Mo et al., 2013).

The type and quantity of the by-products highly depend on photocatalyst properties and operating conditions. When the photocatalyst is irradiated to UV with higher energy, electron-hole pairs can be generated, which can create •OH and O radicals by reacting with O2 and water molecules (Jeong et al., 2013). If the UV radiation to the photocatalyst surfaces is not enough, the generation of by-products will increase (Quici et al., 2010).

Reactors provide contact between gas, photocatalyst, and UV. The efficiency and the rate of PCO reaction can be significantly affected by this reactors (Mansoubi et al., 2017). Various types of photocatalytic reactors with different contact regimes between gas, photocatalyst, and UV have been reported in the literature (Mamaghani et al., 2018; Mansoubi et al., 2017; Mohammadi et al., 2020; Weon and Choi, 2016; Yu et al., 2015). A spouted bed reactor is a kind of fluidized bed in which the gas is introduced through a single orifice from the center of a flat base, instead of a multi-orifice system, resulting in a systematic cyclic pattern of particle movement inside the bed (Sahoo and Sahoo, 2013). A spouted bed reactor provides appropriate fluidization of the particles and adequate exposure to UV (Mansoubi et al., 2018).

However, adding an axially draft tube into the spouted bed reactor has shown potential advantages in the stability and flexibility of the system (Shuyan et al., 2010). The insertion of a draft tube can improve the solid circulation and provide a controlled zone for gas-solid contact by reducing the gas leakage from the spout region to the annulus region (Meng et al., 2020). Also, the studies showed that a porous draft tube is suitable than a non-porous draft tube, when the gas phase has an active role such as photocatalytic reaction (Hosseini et al., 2009).

Health risk assessment is effectively tools to evaluate the hazardous impact of the VOCs on human health over a period of time, which are usually classified as carcinogenic and non-carcinogenic for estimating their human health risks. Health risk assessment is one of the monitoring tools to control community health (Hesam et al., 2022a). The main objective of the present study was to assessment the carcinogenic and non-carcinogenic risk of exposure to by-products of photocatalytic degradation of toluene in a spouted bed reactor Equipped with porous and non-porous draft tube.

Materials and Methods

Experimental set-up

This experimental study was conducted using the following setup (Figure 1). The spouted bed reactor was made of stainless steel with an upper cylindrical section. Schematic of the spouted bed reactor and its dimensions are shown in Figure 2 and Table 1.

The non-porous draft tube was a stainless steel tube located coaxially within the conical section of the reactor. The porous draft tube was made from the sintered metallic filter of stainless steel with a pore diameter of 1 mm and a void fraction of about 40% that its dimensions were similar to a non-porous draft tube. In order to retain particles entrained by the air stream, a stainless steel mesh of standard 60 mesh size was placed at the reactor's outlet as a filter. The irradiation was provided by the UV lamps (Philips, TUV PL-S 9 W/4P), and it was installed in the center of the reactor at a distance of 3 cm from the photocatalyst. The UV lamp had a significant single output peak at the wavelength of 254 nm.

Minimum spouting velocity was determined by Olazar et al. (Olazar et al., 1992) correlation and calculated to be 0.11 m/s. The velocity required to achieve dilute spouting is 1.7 times greater than the minimum spouting velocity (Grace and Epstein, 2011), which in the present study this ratio was proposed to be 1.83. So minimum velocity for dilute spouting was calculated to be 0.21 m/s.

A Nitrogen Gas Cylinder was used to provide the

Table 1. The Dimensions of the Spouted Bed Reactor

Dimension	Symbol	Size (cm)
Total height of the reactor	HT	35
Height of conical section	HC	9
Cylindrical diameter	DC	6
Gas inlet diameter	Di	0.5
Height of entrainment zone	He	1
Height of draft tube	HD	2
Draft tube diameter	DD	1

Table 2. The Specifications of the Particles and Operational Conditions in the Reactor

Photocatalyst (P25)	
Crystalline size (nm)	21
Crystalline structure (%)	80 (A) – 20 (R)
BET- Surface area (m^2/g)	47
Density (g/cm^3)	4.2
Reactor	
Volume (cm^3)	2880
Flow rate (L/min)	0.25
Temperature (oC)	25±1
Relative humidity (%)	40
Inlet toluene concentration (ppm)	200

required contaminated air stream in the setup. The flow rate of air passing through the setup was regulated by a regulating valve and was measured by a rotameter. Air was humidified by passing it through a bubbler. The humidity and temperature of the airstream were monitored by a hygrometer (Proskit NT-312) at the reactor inlet.

Gaseous toluene concentration was made by passing the air through a bottle in which there was a 2 ml vial containing toluene. The ratio of air passing through the bubbler and main line of air determined the toluene concentration. In a mixing chamber, air lines were reached together and 2 airstreams were mixed well. For each experiment, 1.5 g of nanoscale titanium dioxide (Aeroxide ® TiO_2 P25, Evonik Degussa GmbH) was poured into the spouted bed reactor. Table 2 lists the specifications of the particles and operational conditions in the reactor.

The airflow containing an appropriate amount of toluene was passed through the reactor without turning on the lamp. After achieving the steady condition, the source light was turned on. The progress of the reaction was analyzed by detecting toluene concentration at the inlet and outlet of the reactor. The degradation efficiency was calculated using the Eq.1 (Mohammadi et al., 2020):

$$\eta = \left[\frac{C_{in} - C_{out}}{C_{in}}\right] \times 100 \quad \text{(Eq.1)}$$

The Eq.2 was used to determine CO_2 selectivity (Mohammadi et al., 2020):

$$S_{CO_2}(\%) = \left[\frac{CO_2}{7 \times (C_{in} - C_{out})}\right] \times 100 \quad \text{(Eq.2)}$$

Where 7 was number of carbons in toluene and Cin and Cout were the toluene concentration at the inlet and outlet of the reactor, respectively. All concentrations were in ppm.

Sampling and chemical analysis

Gas samples were collected from the sampling ports using a 250 µl gas-tight syringe (Hamilton, Bonaduz, Switzerland). The concentration of toluene was determined by gas chromatography (GC) (Shimadzu GC-17A, Kyoto, Japan) equipped with a flame ionization detector and a split injection system and fitted with a capillary column (DB-17, 30 m by 0.554 mm internal diameter; J & W Scientific, Folsom, Calif.). The column temperature was initially 60°C, and then it was raised to 150°C at the rate of 30°C/min and maintained at that temperature for 5 min. The injector and detector were operated at 180 and 200°C, respectively. Helium was used as the carrier gas at 33 kPa/cm^2.

Gas chromatography mass spectrometry (GC/MS) (Agilent, 7890 GC/5977B MSD, USA) equipped with a flame ionization detector and a HP-5ms capillary column (30 m×0.25 mm inner diameter, 0.25 µm film thickness) was used to identify probable organic by-products. CO_2 at the outlet of the reactor was measured by TES-1370 NDIR CO_2 Meter.

Estimation of Carcinogenic and non-carcinogenic risk

Carcinogenic and non-carcinogenic risks of exposure to toluene and by-products were estimated. Carcinogenic risk is estimated as the excess probability of lifetime cancer risk (LCR), which associated with inhalation exposure to by-products was calculated by Eq.3 and 4:

$$LCR = \mathrm{EC} \times \mathrm{IUR} \quad \text{(Eq.3)}$$

$$EC = \frac{(\mathrm{CA} \times \mathrm{ET} \times \mathrm{EF} \times \mathrm{ED})}{AT} \quad \text{(Eq.4)}$$

EC is exposure concentration (mg/m^3), CA is average concentration of toluene and by-products in the air (mg/m^3 of air), ET is exposure time per day (hours/day), EF is exposure frequency, which indicates the number of exposure days per year (days/year), ED is exposure duration in years, AT is average time (the period in which the exposure is averaged in terms of days) and IUR is unit risk $(mg/m^3)-1$. According to the Integrated Risk Information System of the US EPA, IUR is the upper-bound excess lifetime cancer risk estimated to result from continuous exposure to an agent at a concentration of 1 $\mu g/m^3$ in air (Jalali et al., 2021). After calculating the risk, its amount is compared with the declared permissible limits (Table 3).

For the possible toxic effects of non-carcinogens, the hazard quotient (HQ) was estimated according to Eq.5:

$$HQ_i = \frac{EC_i}{RfC_i} \quad \text{(Eq.5)}$$

Where HQi is the hazard quotient for chemical i that expresses the potential non-carcinogenic health effects resulting from exposure to that chemical and RfCi is the inhalation reference concentration for chemical i (mg/m^3). RfC is an estimate of the daily exposure to the human population that is likely to be without an appreciable risk of deleterious effects during a lifetime (Jalali et al., 2021).

The hazard index (HI) is the summation of HQs for individual contaminants calculated from Eq.6:

$$\mathrm{HI} = \sum HQ_i \quad \text{(Eq.6)}$$

Results

The photocatalytic degradation of toluene in three spouted bed reactors is shown in Figure 3, displayed as a variety of toluene concentrations at the outlet of the spouted bed reactors and the estimation of degradation efficiency with time. Variations of CO_2 concentrations at the outlet of the reactors and CO_2 selectivity in the tested spouted bed reactors is shown in Figure 4. The results of carcinogenic and non-carcinogenic risk assessment of toluene and by-products in the inlet and outlet of three reactors were presented in Table 4.

Table 3. Comparison of Evaluation Results with Permissible Limits

LCR value	Risk
LCR > 0.0001	Certain
0.00001> LCR > 0.0001	Probabilistic
0.000001> LCR > 0.00001	Possible
LCR < 0.000001	No carcinogenic

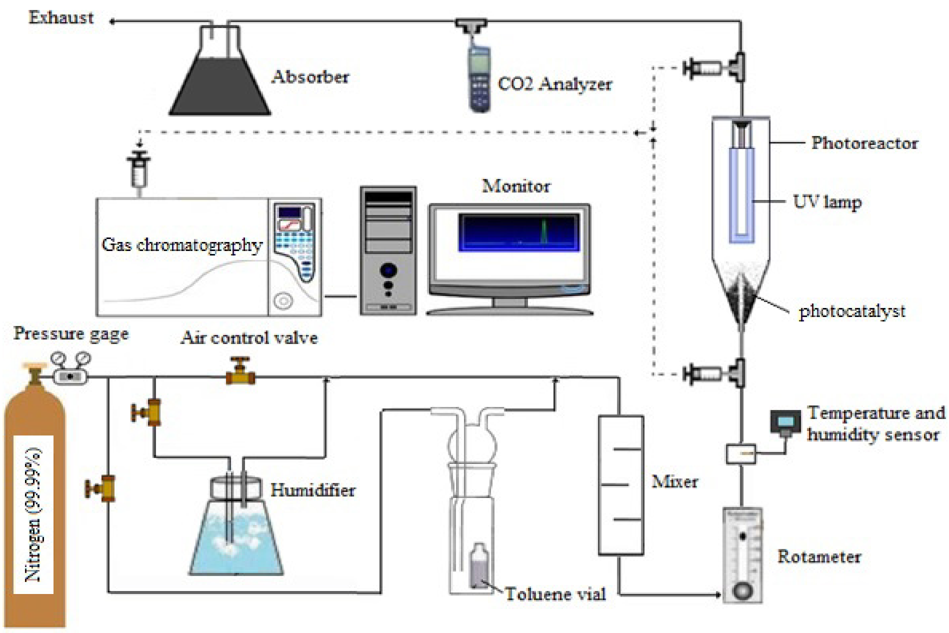

Figure 1. Schematic Diagram of the Experimental Setup

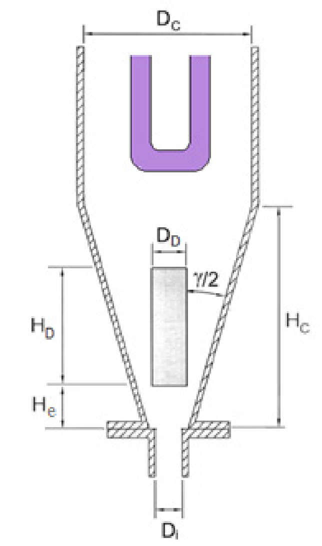

Figure 2. Schematic Diagram of Spouted Bed Reactor

Discussion

The results of photocatalytic degradation of toluene and degradation efficiency show that the degradation of toluene in the spouted bed reactors with draft tube is more than without draft tube; also, in the spouted bed reactor with porous draft tube is more than a non-porous draft tube. The results of degradation efficiency of toluene in the tested spouted bed reactors show that in the first 20 minutes, the spouted bed reactor without a draft tube has a higher degradation efficiency (about 2%) than the reactors with a draft tube. The degradation efficiency then decreases and reverses after 90 minutes. The degradation efficiency decreased from 41.66% to 30.75% within the second 90 minutes. However, the degradation efficiency in the spouted bed reactors with draft tubes does not decrease within 180 minutes. Degradation efficiency in the spouted bed reactors with porous and non-porous

Table 4. Results of Risk Assessment of Exposure to Toluene and by-Products in Spouted Bed Reactors

Spouted bed rectors		Pollutants	CA (mg/m3)	ECcar (mg/m^3)	ECnon-car (mg/m^3)	IUR $(mg/m^3)^{-1}$	RfC (mg/m^3)	LCR	HQ
without draft tube	Inlet	Toluene	746.3		170.31		5		34.1
	Outlet	Toluene	521.94		119.16		5		23.8
		Benzoic acid	0.18		0.04		0.002		20
		Benzaldehyde	1.40		0.32		0.009		35.5
		formaldehyde	1.28	0.12	0.29	0.013	0.0098	0.00156	29.6
		Acetaldehyde	2.90	0.28	0.66	0.0022	0.009	0.000616	73.3
		Cumulative LCR/ HI						0.002176	182.2
with nonporous draft tube	Inlet	Toluene	749.8		171.18		5		34.2
	Outlet	Toluene	394.71		90.11		5		18
		Benzaldehyde	0.60		0.14		0.009		15.2
		HI							33.2
with porous draft tube	Inlet	Toluene	753.7		172.07		5		34.4
	Outlet	Toluene	340.07		77.64		5		15.5

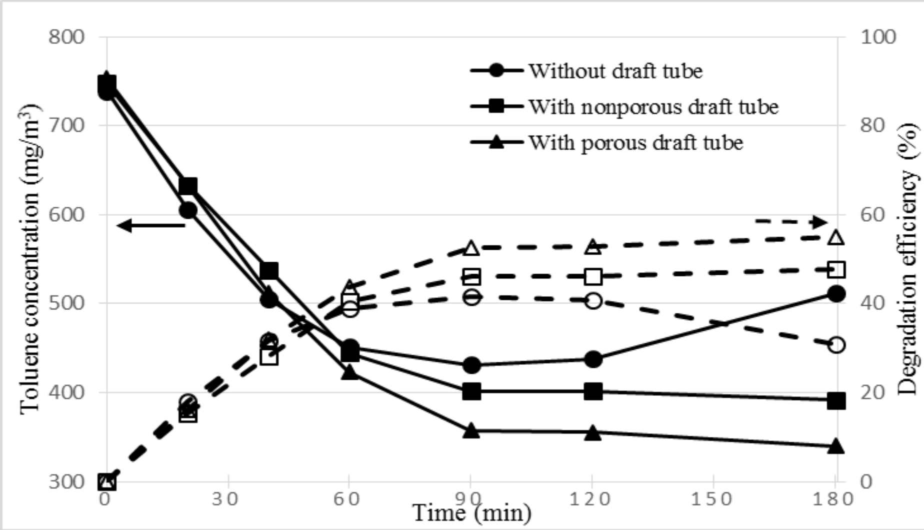

Figure 3. Toluene Concentrations at the Outlet of the Spouted Bed Reactors and the Estimation of Degradation Efficiency

draft tubes was 24.13% and 16.88% higher, respectively, than spouted bed reactor without a draft tube. It seems that the reason for the higher degradation efficiency of toluene in the first 20 minutes, is involving more particles in photocatalytic degradation in the spouted bed reactor without draft tube than the other two reactors. A spouted bed has three different regions: the spout, the fountain, and the annulus. At the stable spouting process, a spout appears at the center of the bed, a fountain appears above the bed surface, and an annulus forms between the spout and wall (Sahoo and Sahoo, 2013). Particles can enter the spout from the annulus at all levels in the spouted bed without a draft tube (Mollick et al., 2018). Therefore, more photocatalyst particles come in contact with toluene and photons, which increases the degradation efficiency. However, the penetrate of particles from the annulus into the spout also has disadvantages, such as the high volume fraction of particles in the annulus region and the lack of photons reaching the photocatalyst particles, and the small mass participation of photocatalyst particles in degradation and forming dead zone (where particles are hard to take part in the particle recirculation) in the reactor (Nagashima et al., 2013). In a spouted bed reactor without a draft tube, the volume fraction of particles in the spout region is higher than the reactors with a draft tube (Nagashima et al., 2013; Wu et al., 2020). It seems a higher volume fraction of particles prevents reaching the UV to all the photocatalyst particles properly, and the mineralization is not completed. Subsequently, by-products are formed, which adhere to the photocatalyst particles leading to the photocatalyst deactivation and reduction of the degradation efficiency (Monazam et al., 2017). Weon and Choi (2016) reported the accumulation of photocatalyst particles in the reactor caused the photon to not reach all the particles and the formation of by-products, which reduces the degradation efficiency.

Studies have also shown in a spouted bed reactor without a draft tube, only the central particles recirculate, and the particles near the wall form a dead zone (Neto et al., 2008). It seems due to the non-participation of a

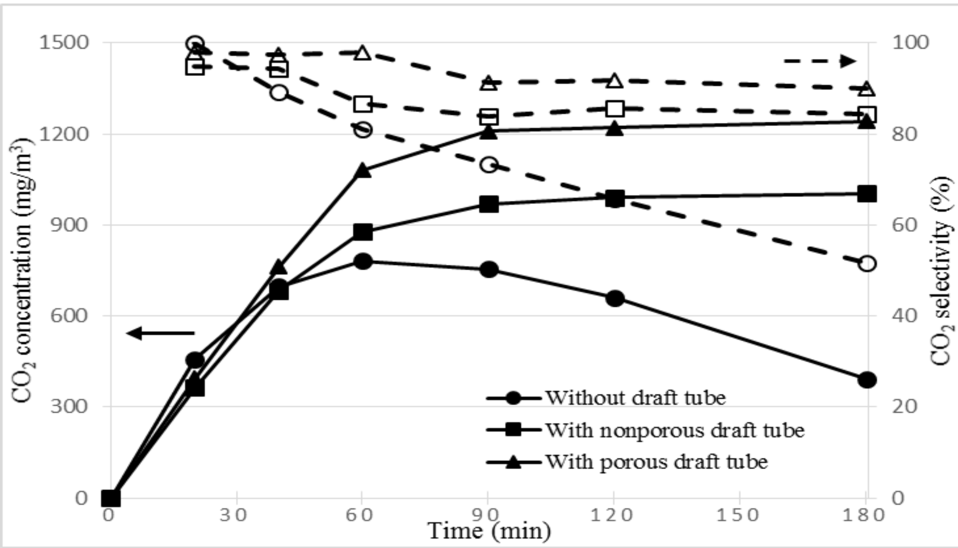

Figure 4. Variations of CO_2 Concentrations at the Outlet of the Reactors and CO_2 Selectivity versus Irradiation Time

dead zone in photocatalytic degradation, the total mass of photocatalyst participating in the reaction is reduced. This causes the photocatalyst to be deactivated rapidly and the degradation efficiency to be reduced.

The insertion of the draft tube in the spouted bed reactor prevents penetrate of particles from the annulus into the spout and causes the particles to recirculate regularly by decreasing the dead zone (Ishikura et al., 2003; Meng et al., 2020). Regular particle recirculation causes all particles to participate in photocatalytic degradation, and by completing the mineralization, prevent the formation of by-products and photocatalyst deactivation.

Comparison of photocatalytic degradation of spouted bed reactors with porous and non-porous draft tubes shows higher degradation efficiency in spouted bed reactor with porous draft tube (about 7.25%). A porous draft tube provides better gas-solid contact than a non-porous draft tube due to the passage of air through the tube porosity (Shuyan et al., 2010). This leads to more toluene contact with the photocatalyst particles and better separation of products. Also, previous studies reported particle circulation rate in the spouted bed with a porous draft tube is higher than a non-porous draft tube (Ishikura et al., 2003; Shuyan et al., 2010), which provides a better gas-solid-photon contact. Hosseini et al., (2009) reported that a spouted bed with a porous draft tube is proper when the gas phase has an active role such as reaction.

The results of formation of CO_2 and CO_2 selectivity show that the formation of CO_2 in the spouted bed reactors with draft tube is more than without draft tube; also, in the spouted bed reactor with porous draft tube is more than a non-porous draft tube. The results of the estimation of CO_2 selectivity show that CO_2 selectivity decreased by 50.8% within 180 min in the spouted bed reactor without a draft tube. It seems, due to incomplete mineralization, toluene is converted to by-products and CO_2 formation is reduced. Beside, detection of by-products by GC-MS confirmed the presence of four by-products (benzaldehyde, benzoic acid, formaldehyde and Acetaldehyde) at the outlet of the spouted bed reactor without a draft tube (Table 4).

In other hand, the average CO_2 selectivity in the spouted bed reactors with porous and non-porous draft tubes were 94.3% and 88.2%, respectively. In these reactors, CO_2 selectivity decreased by only 7.9% and 10.5%, respectively, within 180 minutes. This indicates that mineralization of toluene in reactors with a draft tube is better than reactor without a draft tube, therefore photocatalyst deactivation occurs at a lower rate. This allows the reactor to be used for a longer period of time.

The results show that the CO_2 selectivity in the spouted bed reactor with porous draft tube is higher than the spouted bed reactor with non-porous draft tube (about 6%). The porosity of the draft tube helps air percolation to the annulus and provides a better gas-solid contact. GC-MS results also confirmed the presence of benzaldehyde at the outlet of the spouted bed reactor with a non-porous draft tube, whereas, no by-products were detected at the outlet of spouted bed reactors with porous draft tubes (Table 4).

The better gas-solid contact causes complete degradation of toluene and increases CO_2 formation. Weon and Choi (2016) reported CO_2 generation rate on TiO_2 nanotubes was much higher than that of TiO_2 nanoparticles. This is ascribed to the open channel structure of TiO_2 nanotubes that allows facile O_2 (an essential oxidant needed for mineralization) transfer to the inner tube surface on which the by-products are oxidized and decomposed into CO_2.

The results of carcinogenic and non-carcinogenic risk assessment showed that the carcinogenic risk related to formaldehyde and acetaldehyde in the spouted bed reactor without a draft tube. The lifetime cancer risk of formaldehyde and acetaldehyde in the spouted bed reactor without a draft tube for 30 years were 0.00156 and 0.000616, respectively. Cumulative LCR was 0.002176 that categorized in certain risk. For non-carcinogenic risk, the hazard quotient of inlet toluene was 34.1 in the spouted bed reactor without a draft tube. However the hazard quotients outlet toluene, benzoic acid, benzaldehyde, formaldehyde and acetaldehyde were 23.8, 20, 35.5, 29.6 and 73.3, respectively. The hazard index, summation of HQs, was 182.2 which is much higher than the hazard index of inlet toluene.

No by-products with carcinogenic risk were found in the spouted bed reactor with a non-porous draft tube. In other hand, for non- carcinogenic risk, the hazard quotients of outlet toluene and benzaldehyde in the spouted bed reactor with a non-porous draft tube were 18 and 15.2, respectively, which the hazard index, was 33.2. Although this value is lower than the hazard index in the spouted bed reactor without a draft tube, it is approximately equal to the hazard index of inlet toluene (33.2 vs. 34.2). The by-products have any carcinogenic risk in the spouted bed reactor with a porous draft tube. The hazard quotient of outlet toluene was 15.5 which was lower than the hazard quotient of inlet toluene (HQ_{outlet}=34.4).

The results showed that the incomplete mineralization of toluene in the photocatalytic reactor can produce by-products that are more dangerous than the original contaminants. The suitable design of the photocatalytic reactor can be effective in reducing the formation of by-products. Mo et al. reported that the photocatalytic degradation of toluene can produce by-products such as formaldehyde, methanol, propylene, acetaldehyde, acetone, benzene, acetic acid and benzaldehyde. By adjusting the relative humidity, they were able to reduce the health-related index from 3.3 to 0.6 (Mo et al., 2013).

Detection of four by-products in the spouted bed reactor without a draft tube confirms the mineralization in this reactor is not complete. The insertion of a nonporous draft tube in the spouted bed reactors provided mineralization more complete than in spouted bed reactor without a draft tube by improve the solid circulation and provide a controlled zone for gas-solid contact by reducing the gas leakage from the spout region to the annulus region (Meng et al., 2020). The insertion of a porous draft tube in the spouted bed reactors complete mineralization of toluene by providing appropriate contact between the toluene, photocatalyst, and UV, and prevents the formation of by-products.

In conclusion, The low CO_2 selectivity and the formation of by-products in the spouted bed reactor without a draft tube showed the mineralization of toluene is not complete and toluene is converted to by-products instead of CO_2 and water, which is more harmful than toluene in terms of carcinogenicity and health risk. The insertion of a porous and non-porous draft tube in spouted bed reactors provided mineralization more complete than spouted bed reactor without a draft tube by reducing the dead zone and providing appropriate contact between the toluene, photocatalyst, and UV. Therefore, prevent the formation of dangerous and carcinogenic by-products and will increase the life span of the photocatalyst.

Author Contribution Statement

Ghasem Hesam: Investigation, writing original draft, and writing-review and editing. Rezvan Zendehdel: writing-review, and editing. Somayeh Farhang Dehghan: data collection, analysis and interpretation of results. Hamed Moqtaderi: data collection, analysis and interpretation of results. Mohammad Javad Jafari: Investigation, writing original draft, and writing-review and editing..

Acknowledgements

General

This article is extracted from a PhD dissertation presented by G Hesam and supervised by prof. MJ Jafari. The authors wish to appreciate the School of Public Health and Safety, Shahid Beheshti University of Medical Sciences for their technical and financial support.

Funding Statement

The author(s) disclosed receipt of the following financial support for the research, authorship, and/or publication of this article: This work was financially supported by the School of Public Health and Safety of the Shahid Beheshti University of Medical Sciences.

Ethical Approval

The present study was approved by the Ethics Committee of the Shahid Beheshti University of Medical Sciences through the ethical code: IR.SBMU.PHNS.REC.1399.179.

Availability of data

All data generated or analyzed during this study are included in this published article.

Conflict of Interest

The authors declare that they have no competing interests.

References

Bianchi C, Gatto S, Pirola C, et al. (2014). Photocatalytic degradation of acetone, acetaldehyde and toluene in gas-phase: comparison between nano and micro-sized TiO_2. *Appl Catal B-Environ*, **146**, 123-30.

Chung WC, Mei DH, Tu X, Chang MB (2019). Removal of VOCs from gas streams via plasma and catalysis. *Catalysis Reviews*, **61**, 270-331.

Grace JR, Epstein N (2011). Spouted and Spout-Fluid Beds, Fundamentals and Applications, Cambridge University Press, pp 87-8.

Hesam G, Vahabi Shekarloo M, Atamaleki A, et al. (2022a). Health risk assessment of inhalation exposure to dry fogging of hydrogen peroxide in a dental clinic during the COVID-19 pandemic. *Environ Sci Pollut Res*, **29**, 75338-43.

Hesam G, Zendehdel R, Farhang Dehghan S, Moqtaderi H, Jafari MJ (2022b). Role of porous and non-porous draft tube in photocatalytic degradation of toluene in spouted bed reactors. *Environ Process*, **9**, 62.

Hosseini S, Zivdar M, Rahimi R (2009). CFD simulation of gas–solid flow in a spouted bed with a non-porous draft tube. *Chem Eng Process*, **48**, 1539-48.

Ishikura T, Nagashima H, Ide M (2003). Hydrodynamics of a spouted bed with a porous draft tube containing a small amount of finer particles. *Powder Technol*, **131**, 56-65.

Jalali M, Moghadam SR, Baziar M, et al. (2021). Occupational exposure to formaldehyde, lifetime cancer probability, and hazard quotient in pathology lab employees in Iran: a quantitative risk assessment. *Environ Sci Pollut Res*, **28**, 1878-88.

Jeong MG, Park EJ, Seo HO, et al (2013). Humidity effect on photocatalytic activity of TiO_2 and regeneration of deactivated photocatalysts. *Appl Surf Sci*, **271**, 164-70.

Kim KH, Szulejko JE, Kumar P, et al (2017). Air ionization as a control technology for off-gas emissions of volatile organic compounds. *Environ Pollut*, **225**, 729-43.

Kumar V, Lee YS, Shin JW, et al (2020). Potential applications of graphene-based nanomaterials as adsorbent for removal of volatile organic compounds. *Environ Int*, **135**, 105356.

Li S, Dang X, Yu X, et al (2020). The application of dielectric barrier discharge non-thermal plasma in VOCs abatement: A review. *Chem Eng J*, **388**, 124275.

Malayeri M, Lee CS, Niu J, Zhu J, Haghighat F (2022). Kinetic modeling and reaction mechanism of toluene and by-products in photocatalytic oxidation reactor. *Chem Eng J*, **427**, 131536.

Mamaghani AH, Haghighat F, Lee CS (2018). Photocatalytic degradation of VOCs on various commercial titanium dioxides: Impact of operating parameters on removal efficiency and by-products generation. *Build Environ*, **138**, 275-82.

Mansoubi H, Fatemi S, Mansourpour Z (2018). An efficient photo-catalytic VOC removal process by one-pot synthesized NF/TiO_2 nanoparticles in fluidized-spouted bed reactor. *Part Sci Technol*, **36**, 162-71.

Mansoubi H, Mansourpour Z, Fatemi S (2017). High photocatalytic efficiency of spouting reactor compared with fluidized bed with top irradiation source. *Particuology*, **33**, 123-8.

Marchiori LA, Doubek ÚLR, Ribeiro BMB, Fujimoto TM, and Tomaz E (2019). Photodegradation of cyclohexane and toluene using TiO_2/UV/O3 in gas phase. *Environ Sci Pollut Res*, **26**, 4234-41.

Marycz M, Rodríguez Y, Gębicki J, Muñoz R (2022). Systematic comparison of a biotrickling filter and a conventional filter for the removal of a mixture of hydrophobic VOCs by Candida subhashii. *Chemosphere*, **306**, 135608.

Meng J, Pjontek D, Hu Z, Zhu J (2020). Hydrodynamics of a gas-driven gas-liquid-solid spouted bed with a draft tube. *Can J Chem Eng*, **98**, 2545-56.

Mo J, Zhang Y, and Xu Q (2013). Effect of water vapor on the by-products and decomposition rate of ppb-level toluene by photocatalytic oxidation. *Appl Catal B: Environ*, **132**, 212-8.

Mohamed EF, Awad G (2020). Photodegradation of gaseous

toluene and disinfection of airborne microorganisms from polluted air using immobilized TiO_2 nanoparticle photocatalyst–based filter. *Environ Sci Pollut Res*, **27**, 24507-17.
Mohammadi P, Ghorbani Shahna F, Bahrami A, Rafati AA, Farhadian M (2020). Enhanced photocatalytic activity of hydrothermally synthesised SrTiO3/rGO for gaseous toluene degradation in the air: modelling and process optimisation using response surface methodology. *Int J Environ Anal Chem*, **102**, 222-42.
Mollick PK, Pandit AB, Vijayan PK (2018). Parameters affecting efficient solid circulation rate in draft tube spouted bed. *Ind Eng Chem Res*, **57**, 8605-11.
Monazam ER, Breault RW, Weber J (2017). Analysis of maximum pressure drop for a flat-base spouted fluid bed. *Chem Eng Res Des*, **122**, 43-51.
Moradpour Z, Ghorbani Shahna F, Bahrami A, Soltanian AR, Hesam G (2017). Evaluation of volatile organic compounds at petrochemical complexes in Iran. *Health Scope*, **6**, e62595.
Nagashima H, Suzukawa K, and Ishikura T (2013). Hydrodynamic performance of spouted beds with different types of draft tubes. *Particuology*, **11**, 475-82.
Neto JV, Duarte CR, Murata VV, Barrozo MA (2008). Effect of a draft tube on the fluid dynamics of a spouted bed: Experimental and CFD studies. *Dry Technol*, **26**, 299-307.
Olazar M, San Jose MJ, Aguayo AT, Arandes JM, Bilbao J (1992). Stable operation conditions for gas-solid contact regimes in conical spouted beds. *Ind Eng Chem Res*, **31**, 1784-92.
Quici N, Vera ML, Choi H, et al (2010). Effect of key parameters on the photocatalytic oxidation of toluene at low concentrations in air under 254+185 nm UV irradiation. *Appl Catal B*, **95**, 312-9.
Sahoo P, Sahoo A (2013). Fluidization and Spouting of Fine Particles: A Comparison. *Adv Mater Sci Eng*, **2013**, 1-7.
Shuyan W, Yongjian L, Yikun L, et al (2010). Simulations of flow behavior of gas and particles in spouted bed with a porous draft tube. *Powder Technol*, **199**, 238-47.
Weon S, Choi W (2016). TiO_2 nanotubes with open channels as deactivation-resistant photocatalyst for the degradation of volatile organic compounds. *Environ Sci Technol*, **50**, 2556-63.
Wu F, Che X, Huang Z, et al (2020). Numerical Study on the Gas–Solid Flow in a Spouted Bed Installed with a Controllable Nozzle and a Swirling Flow Generator. *ACS Omega*, **5**, 1014-24.
Yao P, Liu H, Wang D, et al (2018). Enhanced visible-light photocatalytic activity to volatile organic compounds degradation and deactivation resistance mechanism of titania confined inside a metal-organic framework. *J Colloid Interface Sci*, **522**, 174-82.
Yu KP, Lee WMG, Lin GY (2015). Removal of low-concentration formaldehyde by a fiber optic illuminated honeycomb monolith photocatalytic reactor. *Aerosol Air Qual Res*, **15**, 1008-16.